ORIGINAL ARTICLE

Early response assessment after CyberKnife stereotactic radiosurgery for symptomatic vertebral hemangioma by quantitative parameters from dynamic contrast-enhanced MRI

Yongye Chen[1] · Enlong Zhang[2] · Qizheng Wang[1] · Huishu Yuan[1] · Hongqing Zhuang[3] · Ning Lang[1]

Abstract

Purpose The present study aimed to explore the value of DCE-MRI to evaluate the early efficacy of CyberKnife stereotactic radiosurgery in patients with symptomatic vertebral hemangioma (SVH).

Methods A retrospective analysis of patients with spinal SVH who underwent CyberKnife stereotactic radiosurgery from January 2017 to August 2019 was performed. All patients underwent DCE-MRI before treatment and three months after treatment. The parameters included volume transfer constant (K^{trans}), transfer rate constant (K_{ep}), and extravascular extracellular space volume fraction (V_e).

Results A total of 11 patients (11 lesions) were included. After treatment, six patients (54.5%) had a partial response, five patients (45.4%) had stable disease, and three patients (27.3%) presented with reossification. K^{trans} and K_{ep} decreased significantly in the third month after treatment ($p = 0.003$ and $p = 0.026$, respectively). ΔK^{trans} was -46.23% (range, -87.37 to -23.78%), and ΔK_{ep} was -36.18% (range, -85.62 to 94.40%). The change in V_e was not statistically significant ($p = 0.213$), and ΔV_e was -28.01% (range, -58.24 to 54.76%).

Conclusion DCE-MRI parameters K^{trans} and K_{ep} change significantly after CyberKnife stereotactic radiosurgery for SVH. Thus, DCE-MRI may be of value in determining the early efficacy of CyberKnife stereotactic radiosurgery.

Keywords Radiosurgery · Spine · Hemangioma · Multiparametric magnetic resonance imaging

Abbreviations

VH	Vertebral hemangioma
SVH	Symptomatic vertebral hemangioma
SRS	Stereotactic radiosurgery
CR	Complete response
PR	Partial response
PD	Progressive disease
SD	Stable disease
K^{trans}	Volume transfer constant
K_{ep}	Transfer rate constant
V_e	Extravascular extracellular space volume fraction
ICC	Intraclass correlation coefficient
EES	Extravascular extracellular space

Hongqing Zhuang and Ning Lang These authors have contributed equally to this work.

✉ Hongqing Zhuang
    hongqingzhuang@163.com

✉ Ning Lang
    langning800129@126.com

1 Department of Radiology, Peking University Third Hospital, 49 North Garden Road, Haidian District, Beijing 100191, People's Republic of China

2 Department of Radiology, Peking University International Hospital, 1 Life Science Park, Life Road, Haidian District, Beijing 102206, People's Republic of China

3 Department of radiotherapy, Peking University Third Hospital, 49 North Garden Road, Haidian District, Beijing 100191, People's Republic of China

Introduction

Vertebral hemangioma (VH) is the most common benign spinal tumor with an incidence of approximately 11% in adults during autopsy [1]. Most cases of VH are asymptomatic, so VH is usually identified accidentally during imaging examinations. In a small number of patients, VH is identified because of local pain or symptoms and signs of nerve root or spinal cord compression. Approximately 0.9–1.2% of patients with VH present with clinical symptoms [2].

🕿 Springer

Symptomatic VH (SVH) can be treated with vertebrectomy, laminectomy, vertebroplasty, endovascular embolization, or radiotherapy [3–5]. The choice of treatment depends on the patient's specific condition and the severity of clinical symptoms.

Stereotactic radiosurgery (SRS) is guided by images to form a steep dose gradient around the target area to achieve ablative doses and apply highly conformal radiosurgery to the lesion. This approach protects surrounding healthy tissues [6]. As a platform for SRS, CyberKnife can be used to safely and effectively treat SVH [7].

Radiotherapy destroys the SVH vasculature and causes vascular fibrosis, but SVHs that have been successfully treated with radiotherapy do not change significantly when assessed using traditional imaging methods. Specifically, Sakata et al. [8] showed that SVHs did not change significantly after radiotherapy when imaged with CT and plain scan and enhanced MRI, even five years after radiotherapy. Therefore, the efficacy of imaging to evaluate SVHs after radiotherapy is a clinical difficulty.

The microcirculatory changes that occur to the lesion after radiotherapy often occur earlier than general morphological changes that can be observed by imaging. DCE-MRI can noninvasively provide vascular and hemodynamic tumor information *in vivo*, and it can also be used to quantify parameters using the bicompartmental pharmacokinetic model. Otake et al. [9] found that compared with T1-weighted imaging, DCE-MRI can more sensitively detect microcirculatory changes in the bone marrow of the lumbosacral spine after radiotherapy. Therefore, in theory, DCE-MRI has good efficacy for evaluating SVH after radiosurgery; however, no research has been performed to confirm this.

This study retrospectively analyzed the changes in SVH DCE-MRI parameters in patients after CyberKnife SRS combined with changes in patients' clinical symptoms and conventional imaging examination results. We hypothesize that DCE-MRI parameters can be used to evaluate the early efficacy after CyberKnife SRS in patients with SVH.

Materials and methods

Subjects

A retrospective analysis of the case data of patients with spinal SVH who were treated with CyberKnife SRS from January 2017 to August 2019 was performed. This retrospective study was approved by our institutional ethics committees, with waiver of informed consent granted.

The inclusion criteria were as follows: (1) diagnosis of SVH by pathological biopsy or imaging examination and (2) DCE-MRI examination within 1 week before undergoing CyberKnife SRS and 3 months after treatment. The exclusion criteria were as follows: (1) the lesion area that had been subject to surgical resection or radiotherapy before CyberKnife SRS; (2) poor image quality; (3) lesions that could not be evaluated using the revised RECIST, version 1.1; and (4) patient lost to follow-up. Patient information was collected, including age, sex, medical history, lesion location, and clinical symptoms.

Therapeutic plan and efficacy evaluation

Lesions in the thoracic spine or inferior to the thoracic spine were fixed using the BodyFIX® System (Elekta), and lesions in the cervical spine were fixed with a customized thermoplastic mask. The radiotherapist performed an image simulation and target delineation at the CyberKnife System workstation, and the physicist designed the treatment plan using the Multiplan System planning system. X-sight Spine was used to track the lesion. The treatment plan was determined comprehensively based on the tumor location, size, and the tolerable dose of adjacent organs. The prescription dose was 30–35 Gy (5 fractions). The imaging efficacy evaluation was based on RECIST, version 1.1 [10]. RECIST divided the lesions into four groups: complete response (CR), partial response (PR), progressive disease (PD), and stable disease (SD).

DCE-MRI acquisition and analysis

Scanning was performed using the 3.0-T GE Discovery™ MR750 (GE Healthcare) and eight-channel phased array coils. Conventional MRI sequences included sagittal T1-weighted imaging, transverse T2-weighted imaging, sagittal T2-weighted imaging, and sagittal fat suppression T2-weighted imaging.

When a lesion was identified by conventional MRI, DCE-MRI was performed using the three-dimensional volume-interpolated breath-hold examination sequence in the transverse plane to further examine that region. The parameters were as follows: repetition time, 3.9 ms; echo time, 1.7 ms; flip angle, 10°; acquisition matrix, 256 × 160; field of view, 280 × 140 mm; and slice thickness, 2 mm. Thirty-six phases were collected with a temporal resolution of 6 s; the process continued for 216 s. Gadolinium–diethylenetriamine pentaacetic acid contrast agent was injected through an Ulrich medical power injector at a flow rate of 2 ml/s at a dose of 0.1 mmol/kg, and then, 20 ml of physiological saline was injected at the same flow rate.

GenIQ software (GE Medical Systems) was used to measure the data. Based on the extended Tofts model, the parameters included: (1) volume transfer constant (K^{trans}); (2) transfer rate constant (K_{ep}); and (3) extravascular extracellular space volume fraction (V_e) [11]. Changes to DCE-MRI parameters

before treatment compared with the third month after treatment were defined as ΔK^{trans}, ΔK_{ep}, and ΔV_e according to the following equation:

$$\left(\left[\text{pretreatment} - \text{post} - \text{treatment}\right] \div \text{pretreatment}\right) \times 100\%.$$

ROI were delineated at the transverse enhanced T1-weighted image, and the solid components of the tumor were included as much as possible. The analysis was performed independently by two radiologists (EZ and HY) with more than 5 years of experience, and the average value of each parameter was taken as the final measurement result.

Statistical analysis

Patients' clinical information, DCE-MRI parameters, and endpoints were statistically described using mean, median, standard deviation, and percentage. Data that conformed to a normal distribution are presented as mean $\pm$ standard deviation, and data that did not conform to a normal distribution are presented as median and range. The intraclass correlation coefficient (ICC) was used to analyze the agreement between the two physicians. The differences in DCE-MRI parameters before and after radiosurgery were analyzed using the Wilcoxon signed-rank test. p values of <0.05 were considered statistically significant. SPSS 24.0 software (IBM Corporation) was used for statistical analysis.

Results

Patients

Eleven of the 17 patients met the inclusion criteria and were included, with a total of 11 lesions. Five patients were excluded due to surgical resection or radiotherapy before CyberKnife SRS. One was lost to follow-up and was excluded from analyses. Of the 11 included patients, five were male and six were female with an average age of 40.8 ± 14.6 years. Nine patients were diagnosed with SVH by biopsy, and two patients were diagnosed by imaging examination. The median follow-up duration was 10.5 months (range, 7.3–28.0 months), and the mean follow-up duration was 13.4 months. Two lesions were located in the cervical spine, seven lesions were located in the thoracic spine, and two lesions were located in the lumbar spine. All 11 patients showed symptoms of local pain before treatment, and one patient showed neurological symptoms caused by spinal canal stenosis. Basic information of patients is shown in Table 1.

Changes in images and symptoms after treatment

After treatment, there were six patients in the PR group (54.5%, Fig. 1), five patients in the SD group (45.4%, Fig. 2),

Table 1 Basic patient information

Basic information	Number (percentage)
Age	40.8 ± 14.6
Gender	
Male	5 (45.5%)
Female	6 (54.5%)
Location	
Cervical vertebra	2 (18.2%)
Thoracic vertebra	7 (63.6%)
Lumbar vertebra	2 (18.2%)
Sacral vertebra	0 (0%)
Symptoms	
Pain	11 (100%)
Neurological sign	1 (9.1%)
Diagnosis	
Aspiration biopsy	9 (81.8%)
Imaging examination	2 (18.2%)

zero patients in the PD group, and zero patients in the CR group. Three patients (27.3%) presented with reossification (Fig. 2j). Six patients (54.5%) experienced damage to surrounding tissues caused by radiation (Fig. 2i). After treatment, 11 patients experienced different degrees of pain relief, and one patient's neurological symptoms were alleviated.

Changes in DCE-MRI parameters after treatment

The two radiologists' observations were consistent, with an ICC of >0.75. K^{trans} and K_{ep} in the third month after treatment decreased significantly ($p = 0.003$ and $p = 0.026$, respectively). ΔK^{trans} was -46.23% (range, -87.37 to -23.78%), and ΔK_{ep} was -36.18% (-85.62 to 94.40%). K^{trans} decreased after all lesions were treated, and the accuracy of determining pain relief was 100%. K_{ep} decreased in nine patients (81.8%). Representative cases are shown in Figs. 1 and 2. The change in V_e was not statistically significant ($p = 0.213$), and ΔV_e was -28.01% (-58.24 to 54.76%). V_e decreased in six patients (54.5%). Detailed DCE-MRI parameters are shown in Table 2.

Discussion

As a safe and effective treatment, radiotherapy can be used alone or in combination with other treatments [4]. Previous studies have confirmed that traditional radiotherapy can effectively relieve pain in patients with SVH, and the rate of pain relief ranges from 78.4 to 100% [4, 12, 13]. Although radiotherapy can significantly alleviate the clinical symptoms of patients with SVH, there are often no significant
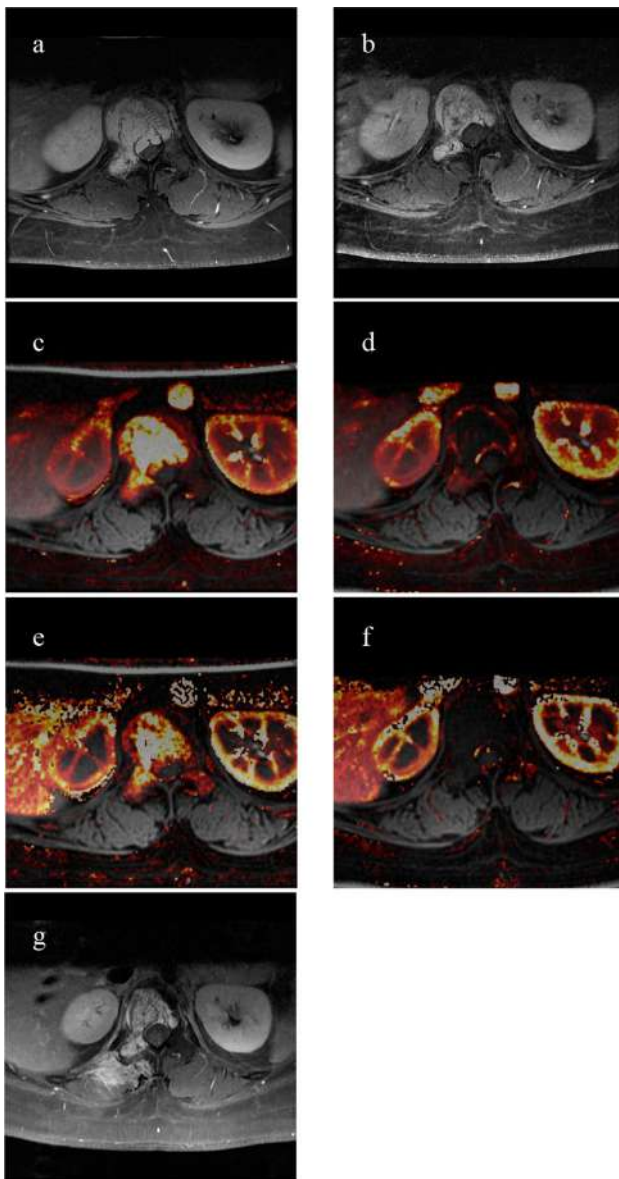
Fig. 1 T12 vertebral hemangioma. **a** Pretreatment axial T1-weighted enhanced MRI showed obvious lesion enhancement in the vertebral body and the right appendix with a surrounding soft tissue mass. **b** In the third month after treatment, axial enhanced MRI showed that the lesion was slightly smaller than before, and enhancement was inhomogeneous with non-enhancing foci. **c** With pretreatment pseudo-color imaging, K^{trans} was 1.869 min^{-1}. **d** With pseudo-color imaging in the third month after treatment, K^{trans} was 0.236 min^{-1}. Thus, compared with pretreatment imaging, K^{trans} decreased by 87.37%. **e** With pretreatment pseudo-color imaging, K_{ep} was 3.907 min^{-1}. **f** With pseudo-color imaging in the third month after treatment, K_{ep} was 0.562 min^{-1}. Thus, K_{ep} decreased by 85.62%. **g** In the 15th month after treatment, axial T1-weighted enhanced MRI showed that the lesion size was further reduced, the surrounding soft tissue mass had almost disappeared, the right erector spinae showed radiation damage, and local muscles were atrophied with obvious enhancement

changes in SVH imaging observations after treatment, even as long as 5 years after treatment [8]. In a case series by Parekh et al. [5], ten SVH lesions did not shrink after being subject to radiotherapy. Heyd et al. [4] reported that most lesions did not show significant changes in imaging characteristics after treatment, and only a small proportion of lesions (approximately 26.2%) demonstrated reossification during long-term follow-up. For this reason, finding a non-invasive method for early detection of treatment outcome is crucial.

CyberKnife SRS may have a better therapeutic effect [14]. Zhang et al. [7] reported the use of CyberKnife SRS to treat five patients with SVH. Four patients experienced relief of clinical symptoms (80%), and two patients demonstrated a reduction in lesion size (40%). Gaviolli et al. [14] also confirmed that CyberKnife SRS is a safe and feasible treatment for SVH. In our study, we found that six lesions had PR (54.5%) during follow-up, and three lesions presented with reossification (27.3%).

Radiotherapy may cause tissue damage, which needs to be differentiated from tumor recurrence [15]. In our study, six patients (54.5%) presented with radiation injury, including radiation-induced osteitis, osteoradionecrosis (Fig. 2i), and soft tissue radiation injury (Fig. 1g), which manifested as increased enhancement in normal tissue outside of the lesion area, but without a soft tissue mass signal.

The changes after treatment are not obvious during traditional imaging examinations, but it can manifest as a decrease in contrast enhancement after treatment and as non-enhancing foci inside the lesion (Figs. 1b and 2b) [16]. Otake[9] suggested that the reduction in enhancement after radiotherapy represents occlusion or fibrosis of capillaries in tumor tissue. A sclerotic rim and reossification appeared in some lesions after treatment in the present study (Fig. 2j), which may suggest that treatment was effective. Some researchers believe that osteolytic metastatic lesions have a sclerotic rim and reossification after radiotherapy, suggesting that it is an effective treatment [17, 18].

DCE-MRI can provide noninvasive, real-time hemodynamic information about tumors *in vivo* and can make up for the shortcomings of traditional imaging methods. At present, studies have used DCE-MRI to evaluate the efficacy of radiotherapy for the treatment of breast cancer, chordoma, and cervical cancer [19–21]. DCE-MRI uses a bicompartmental pharmacokinetic model for quantitative analysis, which assumes that the contrast agent only exists in the intravascular space or the extravascular extracellular space (EES) [11]. Common parameters include K^{trans}, K_{ep}, and V_e. K^{trans} reflects the transfer constant of the contrast agent from the vascular space to the EES, K_{ep} reflects the transfer constant of the contrast agent from the EES to the vascular space, and V_e reflects the volume of the EES [22].

Fig. 2 L2 vertebral hemangioma. **a** Pretreatment axial enhanced ▶ MRI showed obvious lesion enhancement in the vertebral body. **b** In the third month after treatment, axial enhanced MRI showed no obvious changes in lesion size, and the enhancement was inhomogeneous with non-enhancing foci. **c** Pretreatment axial CT imaging. **d** Axial CT imaging at the third month after treatment showed no obvious changes in the lesion. **e** With pretreatment pseudo-color imaging, K^{trans} was 0.249 min^{-1}. **f** With pseudo-color imaging in the third month after treatment, K^{trans} was 0. min^{-1}. Thus, K^{trans} decreased by 39.36%. **g** With pretreatment pseudo-color imaging, K_{ep} was 0.807 min^{-1}. **h** With pseudo-color imaging in the third month after treatment, K_{ep} was 0.618 min^{-1}, and K_{ep} decreased by 23.42%. **i** Twenty months after treatment, axial T1-weighted enhanced MRI showed that the size of the lesion was not significantly different. The range of the low enhancement area was larger than it was previously, a hypointense sclerotic rim was visible around the lesion, and radiation-induced osteitis and osteoradionecrosis appeared. **j** At the 20th month after treatment, there was no obvious change in lesion size when examined by axial CT, and a sclerotic rim and reossification were apparent
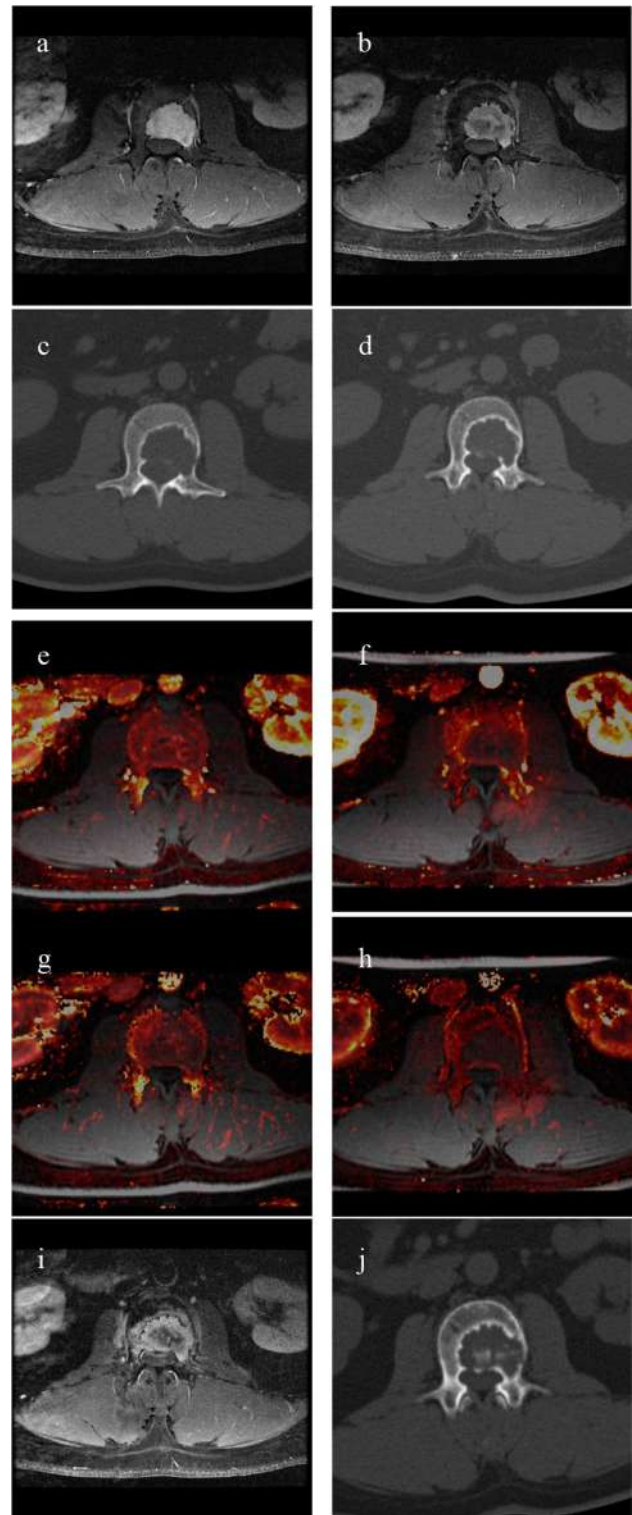
In our study, after SVHs were subject to CyberKnife SRS, K^{trans} and K_{ep} decreased significantly by 46.23% and 36.18%, respectively, while the change in V_e was not statistically significant. The value of K^{trans} is affected by vascular permeability, blood perfusion, and vascular surface area, while K_{ep} is calculated by $K^{trans} \div V_e$ [11, 23]. K^{trans} and K_{ep} are closely related to the state of the tumor microcirculation and angiogenesis. Compared with normal blood vessels, tumor blood vessels have higher permeability and perfusion, which equates to higher K^{trans} and K_{ep} values [24]. Radiotherapy causes destruction to the abnormal blood vessel structure of the tumor, which manifests as a decrease in K^{trans} and K_{ep}.

V_e is the volume of EES per unit volume of tissue. In theory, the blood vessels in tumor tissue are destroyed after radiotherapy, and the volume of the intravascular space decreases. Therefore, the EES volume increases, leading to an increase in V_e. However, V_e is a parameter with a comprehensive impact factor, and it is also affected by blood perfusion. When tumor blood vessels are destroyed after radiotherapy, tumor blood flow decreases, and the amount of contrast agent entering the EES also decreases, resulting in a decrease in V_e [24]. Therefore, V_e is not a stable indicator.

DCE-MRI is a widely used imaging method used to reflect the tumor microcirculation and blood perfusion, and it can provide more information compared with traditional imaging methods. Few previous studies have applied DCE-MRI to VHs, and only one study used DCE-MRI to differentiate between atypical VHs and spinal metastases [25]. This study is the first to use DCE-MRI to explore the changes in SVHs after radiotherapy.

Our study has certain limitations that should be highlighted. First, the number of cases was limited; the sample size was small, and no cases progressed. Therefore, it was impossible to group the lesions to compare the differences in DCE-MRI parameters between the two populations.

Second, not all patients were diagnosed by pathological biopsy; rather, some patients were diagnosed using typical imaging modalities. Third, the follow-up duration was relatively short, with an average follow-up duration of 13.4 months. The long-term prognosis of patients requires further follow-up observation. Fourth, in our study

Table 2 Changes in DCE-MRI parameters of lesions before and 3 months after treatment

Patient no.	Clinico-radiological response				DCE-MRI parameters			Follow-up time (months)
	Pain relief	Efficacy	Reossification	Radiation damage	ΔKtrans	ΔKep	ΔVe	
1	Yes	PR	No	Yes	−87.37%	−85.62%	16.84%	16.5
2	Yes	SD	No	No	−42.51%	−42.38%	4.22%	8.2
3	Yes	PR	No	Yes	−54.11%	5.18%	−49.69%	9.2
4	Yes	SD	Yes	Yes	−39.36%	−23.42%	−32.05%	20.4
5	Yes	PR	No	No	−53.54%	94.40%	−58.24%	10.2
6	Yes	PR	Yes	No	−34.14%	−40.39%	13.25%	14.0
7	Yes	SD	No	No	−69.59%	−50.38%	−32.74%	10.5
8	Yes	PR	Yes	No	−31.88%	−36.18%	14.56%	28.0
9	Yes	PR	No	Yes	−23.78%	−45.47%	54.76%	10.2
10	Yes	SD	No	Yes	−46.23%	−22.04%	−28.01%	7.3
11	Yes	SD	No	Yes	−50.44%	−11.74%	−31.32%	12.8

PR partial response, *SD* stable disease

DCE-MRI was only performed before and 3 months after treatment. The value of DCE-MRI in evaluating long-term efficacy after CyberKnife SRS deserves further research.

Despite some shortcomings, our preliminary attempt to use DCE-MRI to assess the blood perfusion of SVHs provided some valuable results. We conclude that DCE-MRI, as the best noninvasive examination method to reflect tissue hemodynamic information, has good application value in determining early changes in blood perfusion after CyberKnife SRS in patients with SVH. The DCE-MRI parameters K^{trans} and K_{ep} decrease significantly at early stage after treatment. This approach can compensate for the limitations of conventional MRI in evaluating early therapeutic efficacy, especially when changes in tumor morphology are not obvious after treatment. Our study provides valuable information that could inform future clinical practice and guide doctors in developing and planning treatment options.

Compliance with ethical standards

References

1. Pastushyn AI, Slin'ko EI, Mirzoyeva GM (1998) Vertebral hemangiomas: diagnosis, management, natural history and clinicopathological correlates in 86 patients. Surg Neurol 50(6):535–547. https://doi.org/10.1016/s0090-3019(98)00007-x

2. Nguyen JP, Djindjian M, Gaston A, Gherardi R, Benhaiem N, Caron JP, Poirier J (1987) Vertebral hemangiomas presenting with neurologic symptoms. Surg Neurol 27(4):391–397. https://doi.org/10.1016/0090-3019(87)90020-6

3. Acosta FL Jr, Dowd CF, Chin C, Tihan T, Ames CP, Weinstein PR (2006) Current treatment strategies and outcomes in the management of symptomatic vertebral hemangiomas. Neurosurgery 58(2):287–295. https://doi.org/10.1227/01.Neu.0000194846.55984.C8

4. Heyd R, Seegenschmiedt MH, Rades D, Winkler C, Eich HT, Bruns F, Gosheger G, Willich N, Micke O (2010) Radiotherapy for symptomatic vertebral hemangiomas: results of a multi-center study and literature review. Int J Radiat Oncol Biol Phys 77(1):217–225. https://doi.org/10.1016/j.ijrobp.2009.04.055

5. Parekh AD, Amdur RJ, Mendenhall WM, Morris CG, Zlotecki RA (2019) Long-term tumor control with radiotherapy for symptomatic hemangioma of a vertebral body. Spine 44(12):E731-e734. https://doi.org/10.1097/brs.0000000000002973

6. Hall WA, Stapleford LJ, Hadjipanayis CG, Curran WJ, Crocker I, Shu HK (2011) Stereotactic body radiosurgery for spinal metastatic disease: an evidence-based review. Int J Surg Oncol 2011:979214. https://doi.org/10.1155/2011/979214

7. Zhang M, Chen YR, Chang SD, Veeravagu A (2017) CyberKnife stereotactic radiosurgery for the treatment of symptomatic vertebral hemangiomas: a single-institution experience. Neurosurg Focus 42(1):E13. https://doi.org/10.3171/2016.9.Focus16372

8. Sakata K, Hareyama M, Oouchi A, Sido M, Nagakura H, Tamakawa M, Akiba H, Morita K (1997) Radiotherapy of vertebral

hemangiomas. Acta oncologica (Stockholm, Sweden) 36(7):719–724. https://doi.org/10.3109/02841869709001344

9. Otake S, Mayr NA, Ueda T, Magnotta VA, Yuh WT (2002) Radiation-induced changes in MR signal intensity and contrast enhancement of lumbosacral vertebrae: do changes occur only inside the radiation therapy field? Radiology 222(1):179–183. https://doi.org/10.1148/radiol.2221001808

10. Eisenhauer EA, Therasse P, Bogaerts J, Schwartz LH, Sargent D, Ford R, Dancey J, Arbuck S, Gwyther S, Mooney M, Rubinstein L, Shankar L, Dodd L, Kaplan R, Lacombe D, Verweij J (2009) New response evaluation criteria in solid tumours: revised RECIST guideline (version 1.1). Eur J Cancer 45(2):228–247. https://doi.org/10.1016/j.ejca.2008.10.026

11. Tofts PS, Brix G, Buckley DL, Evelhoch JL, Henderson E, Knopp MV, Larsson HB, Lee TY, Mayr NA, Parker GJ, Port RE, Taylor J, Weisskoff RM (1999) Estimating kinetic parameters from dynamic contrast-enhanced T(1)-weighted MRI of a diffusable tracer: standardized quantities and symbols. J Magn Reson Imaging JMRI 10(3):223–232. https://doi.org/10.1002/(sici)1522-2586(199909)10:3%3c223::aid-jmri2%3e3.0.co;2-s

12. Aich RK, Deb AR, Banerjee A, Karim R, Gupta P (2010) Symptomatic vertebral hemangioma: treatment with radiotherapy. J Cancer Res Ther 6(2):199–203. https://doi.org/10.4103/0973-1482.65248

13. Miszczyk L, Tukiendorf A (2012) Radiotherapy of painful vertebral hemangiomas: the single center retrospective analysis of 137 cases. Int J Radiat Oncol Biol Phys 82(2):e173-180. https://doi.org/10.1016/j.ijrobp.2011.04.028

14. Gaviolli E, Sinclair J, Malone S (2020) Case report: cyberknife radiosurgery for the treatment of disabling pain caused by vertebral body hemangioma. J Radiosurg SBRT 6(4):317–319

15. Meixel AJ, Hauswald H, Delorme S, Jobke B (2018) From radiation osteitis to osteoradionecrosis: incidence and MR morphology of radiation-induced sacral pathologies following pelvic radiotherapy. Eur Radiol 28(8):3550–3559. https://doi.org/10.1007/s00330-018-5325-2

16. Hwang YJ, Sohn MJ, Lee BH, Kim SY, Seo JW, Han YH, Lee JY, Cha SJ, Kim YH (2012) Radiosurgery for metastatic spinal tumors: follow-up MR findings. AJNR Am J Neuroradiol 33(2):382–387. https://doi.org/10.3174/ajnr.A2760

17. Barry WF Jr, Wells SA Jr, Cox CE, Haagensen DE Jr (1981) Clinical and radiographic correlations in breast cancer patients with osseous metastases. Skelet Radiol 6(1):27–32. https://doi.org/10.1007/bf00347343

18. Libshitz HI, Hortobagyi GN (1981) Radiographic evaluation of therapeutic response in bony metastases of breast cancer. Skelet Radiol 7(3):159–165. https://doi.org/10.1007/bf00361858

19. Wang C, Horton JK, Yin FF, Chang Z (2016) Assessment of treatment response with diffusion-weighted MRI and dynamic contrast-enhanced MRI in patients with early-stage breast cancer treated with single-dose preoperative radiotherapy: initial results. Technol Cancer Res Treat 15(5):651–660. https://doi.org/10.1177/1533034615593191

20. Santos P, Peck KK, Arevalo-Perez J, Karimi S, Lis E, Yamada Y, Holodny AI, Lyo J (2017) T1-Weighted dynamic contrast-enhanced MR perfusion imaging characterizes tumor response to radiation therapy in chordoma. AJNR Am J Neuroradiol 38(11):2210–2216. https://doi.org/10.3174/ajnr.A5383

21. Zahra MA, Tan LT, Priest AN, Graves MJ, Arends M, Crawford RA, Brenton JD, Lomas DJ, Sala E (2009) Semiquantitative and quantitative dynamic contrast-enhanced magnetic resonance imaging measurements predict radiation response in cervix cancer. Int J Radiat Oncol Biol Phys 74(3):766–773. https://doi.org/10.1016/j.ijrobp.2008.08.023

22. Sujlana P, Skrok J, Fayad LM (2018) Review of dynamic contrast-enhanced MRI: technical aspects and applications in the musculoskeletal system. J Magn Reson Imaging JMRI 47(4):875–890. https://doi.org/10.1002/jmri.25810

23. Yan Y, Sun X, Shen B (2017) Contrast agents in dynamic contrast-enhanced magnetic resonance imaging. Oncotarget 8(26):43491–43505. https://doi.org/10.18632/oncotarget.16482

24. Sun NN, Liu C, Ge XL, Wang J (2018) Dynamic contrast-enhanced MRI for advanced esophageal cancer response assessment after concurrent chemoradiotherapy. Diagn Interv Radiol (Ankara, Turkey) 24(4):195–202. https://doi.org/10.5152/dir.2018.17369

25. Morales KA, Arevalo-Perez J, Peck KK, Holodny AI, Lis E, Karimi S (2018) Differentiating atypical hemangiomas and metastatic vertebral lesions: the role of T1-Weighted dynamic contrast-enhanced MRI. AJNR Am J Neuroradiol 39(5):968–973. https://doi.org/10.3174/ajnr.A5630